

Influence of the Lipid Phase State and Electrostatic Surface Potential on the Conformations of a Peripherally Bound Membrane Protein

María B. Decca,[†] Vanesa V. Galassi,[†] Massimiliano Perduca,[‡] Hugo L. Monaco,[‡] and Guillermo G. Montich^{*,†}

Centro de Investigaciones en Química Biológica de Córdoba (CIQUIBIC, UNC–CONICET), Departamento de Química Biológica, Facultad de Ciencias Químicas, Universidad Nacional de Córdoba, Haya de la Torre y Medina Allende, Ciudad Universitaria, X5000HUA, Córdoba, República Argentina, and Laboratorio di Biocrystallografia, Dipartimento Scientifico e Tecnologico, Università di Verona, Italia

Received: May 3, 2010; Revised Manuscript Received: October 1, 2010

Avian liver bile acid-binding protein (L-BABP) binds peripherally to anionic lipid membranes. We previously showed that in the absence of added salt the binding to 1,2-dimyristoyl-*sn*-glycero-3-phosphoglycerol (DMPG) occurs with changes in the secondary structure, the extent of which depends on the phase state of the lipid. In the present work, we used Fourier transform infrared spectroscopy to study the conformations of L-BABP bound to lipids with phosphoglycerol and phosphatidic acid polar head groups and with different transition temperatures in an aqueous medium with high ionic strength (0.1 M NaCl). When L-BABP was bound to the lipids with saturated acyl chains, DMPG, 1,2-dipalmitoyl-*sn*-glycero-3-phosphoglycerol (DPPG), 1,2-dimyristoyl-*sn*-glycero-3-phosphate (DMPA), and 1,2-dilauroyl-*sn*-glycero-3-phosphate (DLPA), the conformation shifted from a native-like secondary structure to an unfolded state at the temperature of lipid chain melting. The protein was in the native-like conformation when it was bound to the unsaturated 1-palmitoyl-2-oleoyl-*sn*-glycero-3-phosphoglycerol (POPG) in the liquid-crystalline phase. We also measured the electrokinetic surface potential of POPG and DMPG vesicles in the gel and in the liquid-crystalline phase and the protein binding constant to these lipid membranes. We found a correlation indicating that protein unfolding in the interface was due to the increase in the electrostatic surface potential that occurs in the lipid phase transition.

Introduction

A large variety of soluble globular proteins can bind peripherally to lipid membranes. In a simplified picture, it can be considered that the binding is driven by electrostatic interactions between charged domains in the protein and charged lipids in the membrane, by interactions between non polar residues in the protein and in the membrane, or by a combination of these driving forces. Because of the dynamic and complex phase behavior of the lipid membranes and the large conformational space available for peptides, a complete account of protein binding must also take into account the rearrangement of lipids and the conformational changes of the protein as a driving force for the interaction. Examples are the contribution to the free energy of binding from the lipid order perturbation,¹ and the coupling between peptide binding and peptide conformational changes in the interface.^{2–4} From both the biological and physical points of view, the subject is relevant because membrane protein binding usually occurs with changes in the biological activity of the protein,⁵ and the dynamics of the membrane environment allows for a fine modulation of the protein activity.

Liver bile acid binding protein (L-BABP) a member of the lipocalin family, is an excellent experimental system to study the protein conformational changes coupled to membrane binding. This protein does not bind to membranes of the

zwitterionic lipid phosphatidylcholine, it binds to anionic lipid membranes, and the interaction largely decreases by increasing the ionic strength of the medium, indicating that the binding is mainly electrostatic.⁶ Translocation of L-BABP from the solution to the membrane interface at low ionic strength occurs with conformational changes to a partially unfolded state,⁶ and the conformation acquired in the membrane depends on the phase state of the lipid.⁷ L-BABP is an intracellular bile acid transporter in liver.⁸ Recently, it has been shown that the binding of the ligand shifts the equilibrium from the unfolded, membrane-bound apoprotein to the native soluble holo-protein.⁹ This finding was particularly useful to understand the mechanism of ligand transfer.

In a previous work, we have shown that the conformation of L-BABP bound to an anionic lipid membrane is influenced by the phase state of the lipid.⁷ The lipid system used in that work, 1,2-dimyristoyl-*sn*-glycero-3-phosphoglycerol (DMPG), at low ionic strength has a particularly complex thermotropic behavior. The calorimetric transition of the pure lipid is composed of several peaks spanning a wide range of temperature.^{10–12} In both the gel and the liquid crystalline phases, the system is vesicular,¹³ and an intermediate phase is populated over a wide range of temperature. It was proposed that the intermediate phase is a continuous bilayer¹³ or perforated large vesicles.¹⁴ In disagreement with the proposal of a continuous network, it was shown that lipids are not mixed in the intermediate phase.¹⁵ We have also shown that some processes that contribute to the heat uptake are not coincident with the chain melting, as detected by infrared spectroscopy.⁷ Considering the complexity of the thermotropic and structural behaviors of DMPG at low ionic strength, which

* Corresponding author. Tel: +54 351 4334168. Fax: +54 351 4334074. E-mail: gmontich@fcq.unc.edu.ar.

[†] Universidad Nacional de Córdoba.

[‡] Università di Verona.

are the conditions used in our previous work, an important question remains about whether the dependence is specific for that system or if it is a general response of the protein to the state of the membrane. Besides, the physical grounds for the dependence of protein conformation with the lipid phase transition is unknown and requires further investigation. In the present work, we used membrane systems with simpler thermotropic behavior, a sharper melting transition, and lower population of intermediate phases: DMPG, 1,2-dipalmitoyl-*sn*-glycero-3-phosphoglycerol (DPPG), 1,2-dimyristoyl-*sn*-glycero-3-phosphate (DMPA), and 1,2-dilauroyl-*sn*-glycero-3-phosphate (DLPA) in 0.1 M NaCl. We also studied the binding to 1-palmitoyl-2-oleoyl-*sn*-glycero-3-phosphoglycerol (POPG), a lipid that is in the liquid-crystalline state within the whole range of temperature studied here. Using phospholipids with different polar head groups and melting temperature, we demonstrate here that the conformational change of L-BABP is not dependent on a particular lipid and rather depends on a general property of the membrane. We also found in the present work the existence of two well differentiated membrane-bound states for this protein with varying degrees of unfolding, depending on the membrane electrostatic surface potential. We further explored the linkage between lipid organization, protein conformation, strength of binding, and membrane electrostatic surface potential.

Materials and Methods

L-BABP was purified according to Scapin et al.¹⁶ and stored in 2 mM phosphate buffer, pH 7.5, at -70°C . DPPG, DMPG, POPG, DLPA, and DMPA were obtained from Avanti Polar Lipids (Alabaster, AL). D_2O 99.9+% was supplied by Nucleo-eléctrica Argentina S.A. Central Nuclear Embalse, Div. Química y Procesos, NaOD and DCl were from Sigma, and Centricon 100 concentrators were from Amicon (Beverly, MA).

Large Unilamellar Vesicle Preparation. Pure lipids or their mixtures were dissolved in 2:1 chloroform/methanol and dried as a thin film in a glass tube. The film was hydrated and resuspended with 0.1 M NaCl in D_2O to a final concentration of ~ 24 mM lipid. Large unilamellar vesicles (LUVs) were prepared by freeze-thaw and extrusion through polycarbonate filters (pore diameter 100 nm)¹⁷ in an extrusion device from Avanti Polar Lipids. Five cycles of freeze and thaw were done by placing the sample for 10 min in a bath with liquid air and 10 min in a water bath at 60°C . The extrusion step was done at 10°C above the transition temperature of the lipid. Final lipid concentration was measured by quantification of organic phosphate.¹⁸

Fourier Transform Infrared Spectroscopy. The protein was lyophilized from an aqueous solution, dissolved in 0.1 M NaCl in D_2O , and incubated for 24 h at room temperature to allow deuterium exchange of the amide protons. LUVs and pure protein were allowed to equilibrate at 10 – 15°C for 15 min and mixed to reach a final total lipid-to-protein molar ratio ranging from 100:1 to 200:1. Typically, lipid concentration was ~ 20 mM, and protein concentration was between 0.1 and 0.2 mM. Spectra were recorded in a Nicolet Nexus spectrometer using a thermostatted demountable cell for liquid samples with CaF_2 windows and $75\ \mu\text{m}$ Teflon spacers. The spectrometer was flushed with dry air to reduce water vapor distortions in the spectra. Normally, 50 scans were collected for both the background and the sample at a nominal resolution of $2\ \text{cm}^{-1}$. The temperature in the cell was controlled with a circulating water bath. The temperature setting in the bath was manually increased in steps of $\sim 5^{\circ}\text{C}$. The actual temperature in the

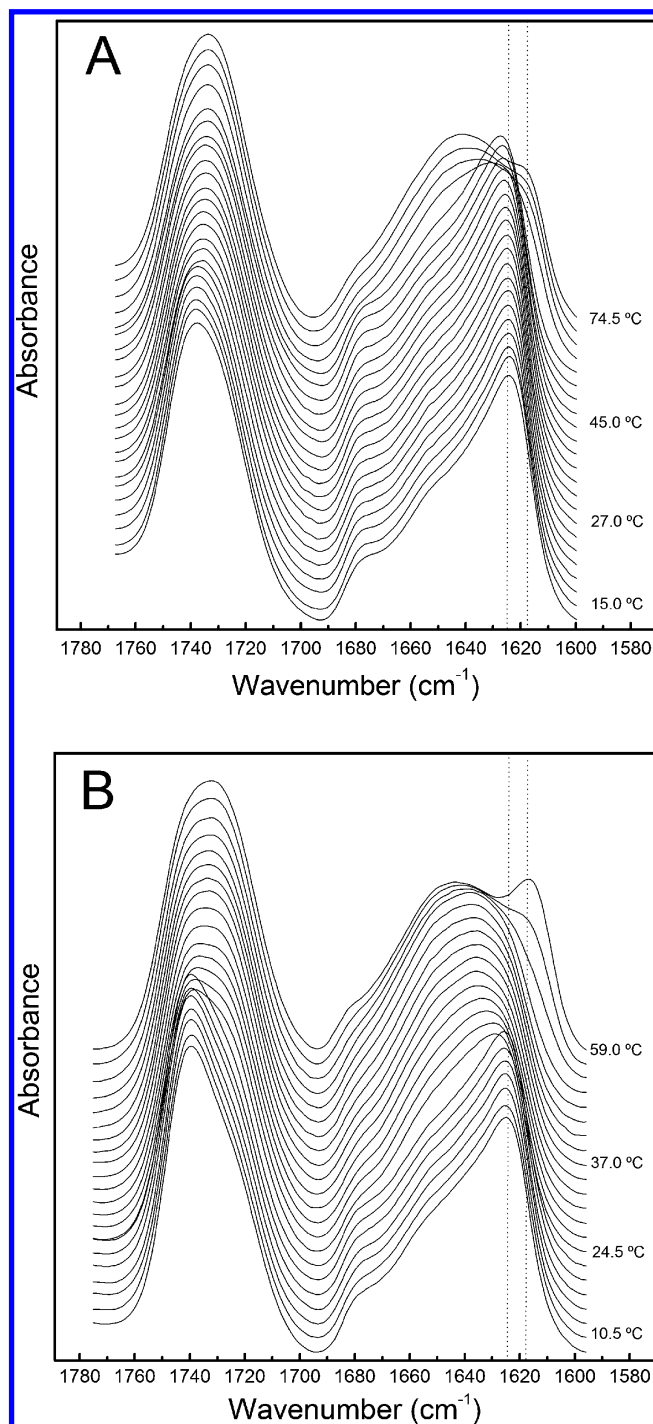


Figure 1. Infrared spectra of the amide I' of L-BABP and C=O stretching band of lipid carbonyl groups as a function of temperature. (A) Protein in the presence of DMPC LUVs. (B) Protein bound to DMPG lipid membranes. Samples were prepared in D_2O and contained 24 mM DMPC or lipid, 0.21 mM L-BABP, and 0.1 M NaCl, pH 6.8.

sample, measured with a thermocouple inserted in the cell, increased continuously with a scan rate of $\sim 0.5^{\circ}\text{C}/\text{min}$. The acquisition of a spectrum at a given nominal temperature (that is, the acquisition of the 50 individual scans) spanned 1 min and a change in the temperature of $\sim 0.5^{\circ}\text{C}$. Data plotted in Figures 1 and 2 correspond to the temperature readings in the midpoint of that segment of time. We eliminated the contribution of the D_2O in the amide I' region by subtracting the absorbance of the 0.1 M NaCl solution in D_2O acquired at the corresponding temperature. A linear baseline was defined between 1600 and $1690\ \text{cm}^{-1}$, and the bands were normalized between these limits.

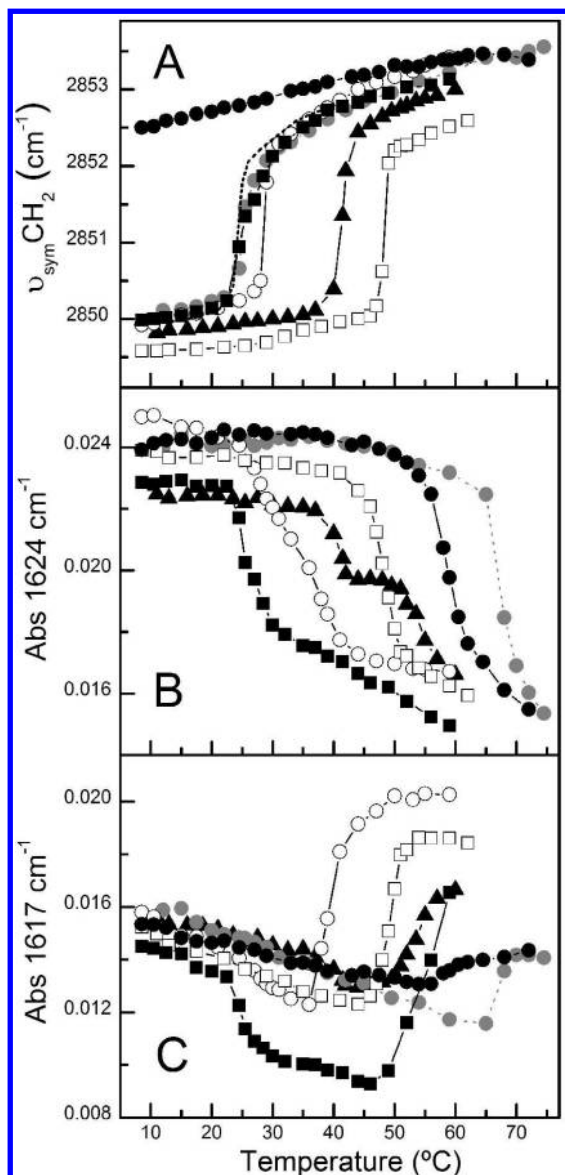


Figure 2. Infrared spectral parameters of lipids and L-BABP in the lipid-protein complexes as a function of the temperature. (A) Position of $-\text{CH}_2-$ stretching bands of lipid hydrocarbon chain. (B) Intensities of the amide I' band of L-BABP at 1624 cm^{-1} . (C) Intensities of the amide I' band of L-BABP at 1617 cm^{-1} . Samples were prepared in D_2O and contained 24 mM lipid, 0.21 mM L-BABP, and 0.1 M NaCl, pH 6.8. ●, POPG; ■, DMPG; ▲, DPPG; ○, DLPA; □, DMPA; gray circle, DMPG. Dotted line in panel A is the position of the $-\text{CH}_2-$ stretching band of DMPG in absence of bound protein.

The Fourier transform infrared (FTIR) measurements as a function of the temperature were repeated in three separate samples for each lipid. One of the three identical results is shown in Figures 1 and 2.

Filtration Binding Assay. Lyophilized protein was dissolved in 0.1 M NaCl aqueous solution. LUV and pure protein were preincubated for 15 min at the desired temperature and mixed to reach the desired lipid/protein molar ratio. Samples containing pure protein and lipid-protein mixtures were preincubated for 30 min at 13 or 37 °C, loaded in the upper chamber of Microcon YM100 concentrators (Amicon), and spun down at 14 000g at 13 or at 37 °C until 60–70% of the initial volume was eluted. The protein concentration in the initial sample and in the eluted fraction was quantified, recording the absorbance spectra in the UV region and measuring the absorbance at 280 nm. Protein concentration in binding assays was $3.8\text{ }\mu\text{M}$, and lipid concen-

tration varies from 0.1 to 0.6 mM. YM100 filters allow the passage of the soluble protein (eluted fraction) retaining lipid vesicles and membrane-bound protein. Filtration binding assays were performed at constant protein concentration ($3.8\text{ }\mu\text{M}$) with varying the lipid concentration in the system. Lipid was not detected in the eluted material.

Electrokinetic Potential. The Electrokinetic potential was measured by electrophoretic light scattering (ELS) in a Delsa Nano C instrument from Beckman Coulter, equipped with the transparent electrode technology for forward scattering. This enabled us to obtain accurate ζ potential values regardless of the sample concentration or conductivity. The chamber was loaded with extruded vesicles, 1 mM total lipid concentration, in 0.1 M NaCl. Zeta potential, ζ , was calculated from electrophoretic mobility using Helmholtz–Smoluchowski equation

$$\zeta = \frac{\eta\mu}{\epsilon\epsilon_0} \quad (1)$$

where μ is the electrophoretic mobility, η is the dynamic viscosity of the suspension (assumed to be equal to water), and ϵ and ϵ_0 are the dielectric permittivity of the suspension and of vacuum respectively. Experiments were carried out at different temperatures through Peltier accurate temperature control.

Dynamic Light Scatter Measurement. Particle size was measured in a Nicomp 370 dynamic light scattering instrument (Nicom Particle Sizing Systems, Santa Barbara, CA) equipped with a 30 mW laser (632.8 nm wavelength). The scattered light intensity detected at a 90° angle was treated using the Gaussian or multimodal Nicomp analysis depending on the polydispersity of the samples. The data presented correspond to the volume-weighted distributions. The mean diameters shown are averages of three measurements performed on different samples for periods of time long enough (from 30 min to 4 h) to collect statistically reliable data.

Differential Scanning Calorimetry. Thermograms were obtained in a VP-DSC scanning calorimeter from MicroCal (Northampton, MA). The reference cell was filled with 0.1 M NaCl solution, and a 26 psi pressure was applied to both cells. A scan rate of $30\text{ }^\circ\text{C/h}$ was used for all experiments. DMPG concentration was 0.4 mM, and protein concentration varies from 2 to $8\text{ }\mu\text{M}$. Differential scanning calorimetry (DSC) experiments were repeated in two separate samples for each experimental condition.

Results

FTIR: Lipid Phase Transition and Conformational Changes of L-BABP. We studied the interactions of L-BABP with different lipid membranes in the presence of 0.1 M NaCl using FTIR spectroscopy. We included anionic lipid membranes with two different polar head groups, phosphatidylglycerol and phosphatidic acid, and with different transition temperatures for the gel to liquid-crystalline phase transition. Infrared spectroscopy is suitable to study both protein conformation and lipid membrane organization. We studied the changes in protein secondary structure by analyzing the amide I' band (between 1600 and 1700 cm^{-1} in D_2O solutions), mainly due to the $\text{C}=\text{O}$ stretching of the peptide bonds.¹⁹ The gel to liquid-crystalline lipid phase transition was studied by the position of $-\text{CH}_2-$ stretching bands (between 2890 and 2850 cm^{-1}), which are sensitive to the number of trans-gauche isomerizations of the hydrocarbon chain.^{20–22} According to the measured binding constants (described in following sections), all FTIR measure-

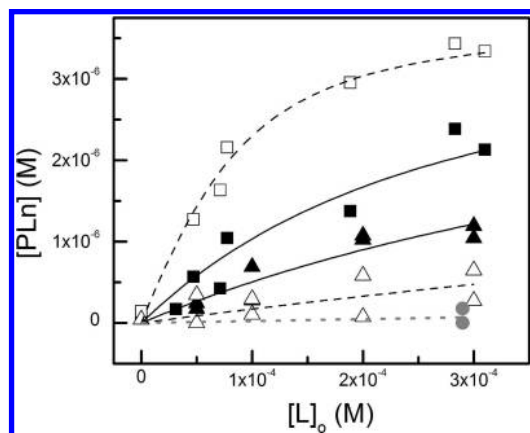


Figure 3. Binding of L-BABP to LUV vesicles of DMPG and POPG. The concentration of membrane-bound protein, $[PLn]$, was plotted against the total available lipid concentration, $[L]_0$, taken as half of total lipid concentration because protein interacts only with the external hemilayer. Lines are the best fit of experimental data to eq 5. Samples contained $3.8 \mu\text{M}$ L-BABP, 0.1 M NaCl, pH 6.8. \square , DMPG at 37°C ; \blacksquare , DMPG at 13°C ; \triangle , POPG at 37°C ; \blacktriangle , POPG at 13°C ; gray circle, DMPC at 37°C .

ments in the presence of anionic lipids were done under experimental conditions where the protein was bound to the lipid membrane and the infrared spectra corresponded to a membrane-bound protein. In addition, increments of up to five-fold in the lipid concentration produced no changes in the infrared spectra of L-BABP, further indicating that there was no contribution to the spectra from the free L-BABP in solution. The infrared spectrum of native L-BABP in solution was already described:⁶ Fourier self-deconvolution and second derivative revealed major bands at 1624 and 1632 cm^{-1} assigned to extended and antiparallel β -chain, respectively; a band at 1653 cm^{-1} was assigned to the α -helical structure, and a band at 1642 cm^{-1} was assigned to unordered structures. Minor bands at 1662 , 1671 , and 1680 cm^{-1} corresponding to turns and bends were also found.

L-BABP does not bind 1,2-dimyristoyl-sn-glycero-3-phosphocholine (DMPC) vesicles according to filtration binding assays (see below, Figure 3). Therefore, this system is an appropriate control for the behavior of L-BABP in the presence of a noninteracting lipid membrane. Figure 1A shows the amide I' band of L-BABP in the presence of zwitterionic DMPC membranes at different temperatures in 0.1 M NaCl D_2O solutions. The FTIR spectra and their changes with temperature were the same as those for the protein in solution:⁶ the shape of the amide I' band remained unchanged up to 65°C . Above this temperature, a cooperative unfolding was observed, evidenced by a decrease in the bands corresponding to β structure (1624 cm^{-1}), an increase in unordered structures (1640 cm^{-1}), and the appearance of bands at 1617 and 1682 cm^{-1} , characteristic of intermolecular contacts of unfolded, aggregated structures.²³ These results are in agreement with those observed for L-BABP in solution, which has a cooperative transition to the unfolded state at 75°C . Below this point, the structure of L-BABP, according to the IR spectral shape, remains unchanged within the temperature range.⁶ Spectral changes observed between 10 and 70°C for the protein in solution are negligible as compared with the spectral changes induced by the lipid phase transition described below.

Figure 1B shows the amide I' band of L-BABP bound to DMPG membranes at different temperatures. The spectra show the stretching band of carbonyl groups in DMPG (between 1700 and 1800 cm^{-1}) that are also sensitive to the phase state of the

lipid.²⁴ The spectra of L-BABP bound to DMPG membranes in the gel phase in 0.1 M NaCl were similar to the FTIR spectra of the free protein in solution (Figure 1B, 15 – 22.5°C). When the membrane was in the liquid-crystalline phase instead, the protein acquired a partially unfolded conformation, similar to that previously described for fluid phases at low ionic strength⁷ (Figure 1B, $T > 30^\circ\text{C}$). Because we cannot distinguish if the conformation acquired in the liquid phase of other lipids is a partially or completely unfolded state (see below), we will refer to any state that does not show a native spectrum as "unfolded".

Figure 2A shows the thermotropic phase transition of the lipids as detected by changes in the position of the $-\text{CH}_2-$ stretching band in the lipid–protein complexes. The sharp changes in the band position as a function of the temperature evidenced the gel to liquid-crystalline phase transition at 25.0°C for DMPC, 25.5°C for DMPG, 28.6°C for DLPA, 41.5°C for DPPG, and 48.5°C for DMPA. POPG membranes were in the liquid-crystalline phase within the temperature range. Except for DMPG, these curves were identical to those obtained for the pure lipid (not shown). The onset of the curve for the DMPG–protein complexes was coincident with the pure lipid, but at temperatures above the transition midpoint, the lipid was slightly more ordered in the lipid–protein complexes. For comparison, the behavior of pure DMPG is shown with dashed line in Figure 2A.

The changes in the spectral shape of L-BABP bound to different lipids are shown in Figure 2B, where the absorbance at 1624 cm^{-1} is plotted as a function of the temperature. The larger values of absorbance at the left of the plot are representative of native-like spectra. The acquisition of an unfolded state appears in the Figure 2B as a decrease in absorbance at 1624 cm^{-1} . For DMPG, the transition between native-like and unfolded structure of L-BABP occurred within a narrow temperature range and with a midpoint at 25.0°C , which is the same temperature as the gel to liquid-crystalline transition of DMPG in the complexes. The band at 1617 cm^{-1} appeared above 45°C (Figure 2C), indicative of the self-aggregation of unfolded strands.²³ This aggregation occurred at a temperature of $\sim 30^\circ\text{C}$ below the temperature for the unfolding and aggregation of the protein in solution⁶ or in the presence of DMPC membranes. Protein aggregation in the interface could be facilitated both by a decreased thermal stability of the bound protein and by the increased local, interfacial concentration.

The behavior of L-BABP bound to other anionic lipids with different polar headgroup or hydrocarbon chain composition, shown in Figure 2B,C, was similar to that observed in DMPG. In all cases, the unfolding revealed by the decrease in the band at 1624 cm^{-1} was coincident with the lipid phase transition. This was at 40°C in DPPG and at 47°C in DMPA. In DLPA, the transition was broader, with a midpoint at 35°C , that is 5°C above the lipid phase transition, but the onset of the change was at 25°C , still in agreement with the transition of DLPA. The protein aggregation, detected by the increase in the band at 1617 cm^{-1} , also occurred at lower temperatures than the protein in solution. Two groups of lipids can be distinguished according to the extent and the temperature of aggregation: for DMPG and DPPG, the protein aggregation occurred at temperatures well above the temperature of partial unfolding. This means that there is a range of temperature in which L-BABP remains partially unfolded in the interface without aggregation. For DMPA and DLPA instead, the aggregation occurred at temperatures immediately above protein unfolding, and the extent of aggregation was higher than that for DMPG and DPPG membranes. Apparently, in the interfaces with phosphatidic acid

TABLE 1: Binding Constant, K_a , for the Association of L-BABP to Different Lipid Membranes

lipid	T (°C)	protein conformation	$K_a \times 10^{-5}$ (M ⁻¹)	% bound protein	ΔG (kcal/mol) ^a	ζ (mV)	$zF\zeta$ (kcal/mol)	
							$z = +1$	$z = +5$
DMPG	13	N	0.90 ± 0.1	97.4	-8.76	-41 ± 2	-0.95	-4.75
DMPG	37	U	5.70 ± 0.7	99.6	-10.63	-58 ± 2	-1.34	-6.7
POPG	13	N	0.35 ± 0.3	93.3	-8.22	-8.5 ± 0.5	-0.42	-2.1
POPG	37	N	0.11 ± 0.3	80.8	-8.14	-7 ± 1^b	-0.39	-1.95
DMPG 5% DMPC	37	N	1.50 ± 0.5	98.3	-9.8	-45 ± 1	-1.04	-5.26

^a Calculated as $\Delta G = -RT \ln(K_a[W])$, where $[W]$ is the molar concentration of water. ^b Measured at 33 °C.

polar headgroup in the liquid state, the unfolded aggregated state was directly populated from the native, with a small amount, if any, of partially unfolded state.

Association of L-BABP with POPG lipid membranes in 0.1 M NaCl showed particular characteristics. No changes in the infrared spectra of L-BABP were observed after binding to POPG, even when this membrane was in liquid-crystalline phase at the temperatures studied. This must be compared with DMPG, in which L-BABP was unfolded in the liquid phase. The POPG-bound protein produced the same infrared spectral shape as L-BABP in solution up to 55 °C. Above this temperature occurred the cooperative unfolding and aggregation. As for the other lipid membranes, association with POPG also produced a decrease in the thermal stability, helping the aggregation at temperatures lower than those for the free protein in solution.

Considering that no changes were observed for the protein in solution below 70 °C, it is concluded that the changes described in Figure 2, except those corresponding to protein aggregation, were due to the changes in the membrane properties upon lipid phase transition.

Measurement of the Binding Constant by Filtration Assay.

We measured the binding constants of L-BABP to DMPG and POPG lipid membranes at 13 and 37 °C, corresponding to temperatures below and above the phase transition of DMPG, respectively, and to the liquid phase of POPG. We measured the concentration of free protein by filtration binding assay. (See the Materials and Methods section.) We considered a Langmuir binding isotherm, where the protein binds to n lipid molecules



The association constant expressed in molar unit concentrations is

$$K_a = \frac{[PLn]}{[P][Ln]} \quad (3)$$

or

$$K_a = \frac{[PLn]}{([P]_0 - [PLn])([L]_0/n - [PLn])} \quad (4)$$

For a given total lipid and total protein concentration, the membrane-bound protein concentration can be calculated

$$[PLn] = \frac{[P]_0 + [L]_0/n + 1/K_a - \sqrt{([P]_0 + [L]_0/n + 1/K_a)^2 - 4[P]_0[L]_0/n}}{2} \quad (5)$$

$[PLn]$ is the membrane-bound protein concentration, $[P]$ is the concentration of free protein, $[P]_0$ is the analytical or total protein concentration, $[L]_0$ is the total available lipid concentration (half of the total analytical lipid concentration, if we assume that the protein interacts only with the external hemilayer), and n is the number of lipid molecules involved in the binding of one protein molecule. K_a values were obtained by nonlinear regression fitting of eq 5 to the experimental data. A value of $n = 20$ lipids was used, considering the average L-BABP diameter in comparison with average lipid molecular area.²⁵

The measurements of binding constants served two purposes. On one side, we used the measured binding constants to estimate the amount of bound protein in the FTIR experiments. On the other side, the variation of binding strength in different interfaces helped us to understand the nature of these interactions. Under conditions of relatively low concentration of lipid and protein, as in the filtration binding assays, a fraction of protein can be found free in solution. At the same lipid/protein molar ratio, the equilibrium can be shifted, increasing the amount of bound protein if the amount of aqueous phase is reduced or, in other words, if the lipid concentration is increased. This is a typical condition in an FTIR experiment, in which the measurements require samples containing ~20 mM total lipid concentration. Because it is technically difficult to perform separation binding assays by either filtration or sedimentation under these conditions, we measured the binding constant at low lipid concentration and calculated the amount of membrane-bound protein for the conditions of FTIR experiments according to eq 5. Figure 3 shows the amount of membrane-bound protein as a function of the total accessible lipid. Binding constants of L-BABP in POPG and DMPG membranes at 13 and 37 °C are shown in Table 1. According to the K_a values and using eq 5 (column 4 in Table 1), we calculated the percentage of protein associated with lipid membranes at the total lipid and total protein concentrations used in the FTIR experiments: $[P]_0 = 2.1 \times 10^{-4}$ M and $[L]_0 = 1.2 \times 10^{-2}$ M. We concluded that a high percentage of protein was bound to the membranes in all FTIR experiments with anionic DMPG and POPG, without significant contribution to the spectra from free protein in solution.

The binding constant slightly decreased with the increase in temperature for POPG membranes (Table 1, column 4). If we consider that POPG is always in the liquid-crystalline phase within this temperature range, then we can conclude that the variation was due to the normal thermodynamic dependence of this equilibrium constant with the temperature. We observed a comparatively large increase in the binding constant to DMPG membranes with temperature. In this case, the variation in the strength of binding must also be due to the different properties of the membrane in the gel as compared with the liquid-crystalline phase. It must be noticed that even when they are both in the liquid phase at 37 °C, binding to DMPG is stronger than that to POPG.

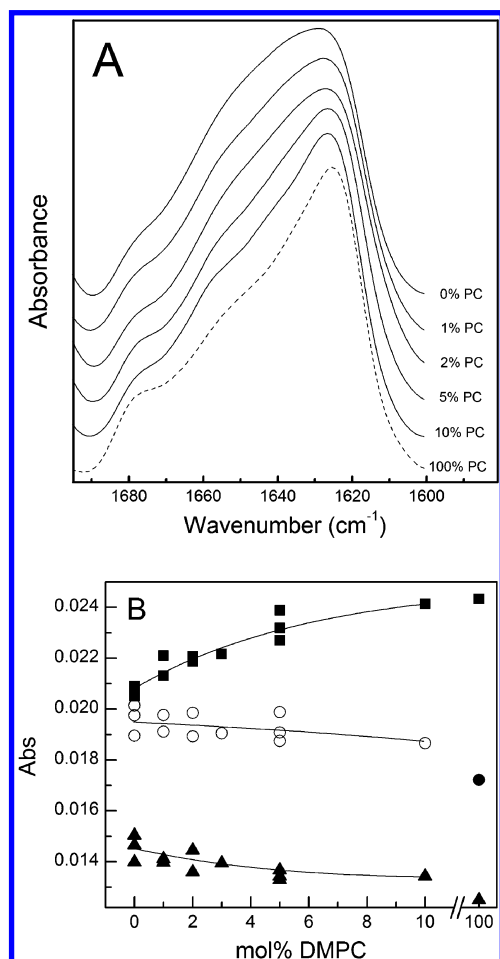


Figure 4. Infrared spectra of L-BABP bound to lipid membranes with different proportions of DMPC in DMPG. Panel A: Amide I' of L-BABP bound to LUVs, the percentage of DMPC in the membrane is indicated next to the spectra. Panel B: infrared absorbances of L-BABP measured at: ■, 1624; ○, 1640; and ▲, 1654 cm⁻¹ as a function of the DMPC content. Measurements were at 37 °C. Samples were prepared in D₂O and contained 20 mM total lipid (DMPG + DMPC), 0.2 mM L-BABP, and 0.1 M NaCl, pH 6.8.

Dependence of Protein Conformation with the Electrostatic Surface Potential. Electrostatics play a role in the binding,⁶ and molecular dynamic simulations indicate that the electric field in the membrane can influence the protein conformation.²⁵ To explore if electrostatics mediate the influence of the lipid phase state on the protein binding and conformation, we studied the binding to interfaces where the surface charge density was decreased by including the zwitterionic lipid DMPC and measured the electrokinetic surface potential, ζ , of POPG, DMPG, and DMPG–5%DMPC.

FTIR spectra of L-BABP bound to DMPG/DMPC membranes in the liquid-crystalline phase at 37 °C are shown in Figure 4A. The variation of the spectral shape as a function of DMPC content is shown in Figure 4B. When the proportion of DMPC was increased, the spectra progressively acquired the native shape. This result is in agreement with the proposal that membrane surface potential modulates protein conformation at the interface. The measurements of ζ of DMPG and DMPG–5%DMPC as a function of temperature are shown in Figure 5, and the more relevant values are included in column 7 of Table 1. The dependence of ζ with temperature was not linear and followed a broad sigmoidal shape. The midpoint for the transitions shown in Figure 5 is about at the temperature for the lipid phase transitions, strongly suggesting that changes in

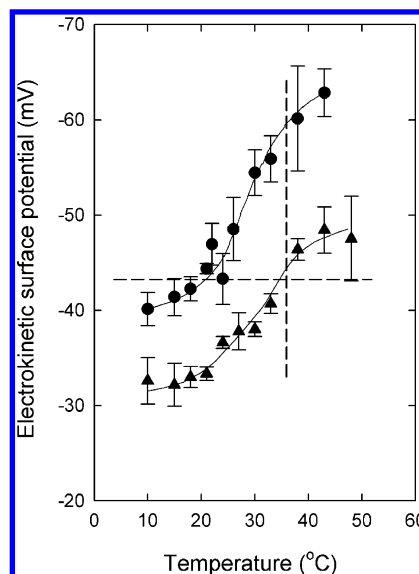


Figure 5. Electrokinetic surface potential, ζ , of LUVs as a function of the temperature. ●, LUVs of pure DMPG; ▲, LUVs of DMPG–5%DMPC. Samples contained 0.1 M NaCl. Vertical line is to emphasize the decrease in ζ at 37 °C when DMPC was included in the LUVs. Horizontal line is to emphasize that pure DMPG membranes in the gel phase have the same ζ as DMPG–5%DMPC membranes in the liquid crystalline phase.

ζ are coupled to changes in the lipid phase state. It must be noticed that in POPG membranes that are in the liquid phase within the whole temperature range, ζ was constant (shown in column 7 Table 1). We found that DMPG and DMPG–5%DMPC membranes have lower ζ potential in gel phase than in liquid-crystalline phase and that POPG membranes have lower ζ potential than DMPG membranes.

Then, a correlation among membrane electrostatic surface potential (at least for the pure lipid vesicles), strength of binding, and protein conformation can be established. It can be seen in Figure 5 and Table 1 that the membrane-bound, native-like protein occurred under conditions in which the pure lipid vesicles have the same low surface potential. Unfolded state was observed in membranes with higher values of surface potential, this is DMPG in the liquid-crystalline phase.

Influence of the Protein on the Membrane Properties. We also studied the changes in the lipid membrane due to the binding of L-BABP. Figure 6 shows the heat capacity as a function of temperature for pure DMPG and DMPG/L-BABP mixtures in different proportions. The transition of the pure lipid included several components: a sharp peak at 24.5 °C and broader peaks at 25, 27, and 29 °C. This profile is similar to that described by Zhang et al.¹⁰ and Riske et al.²⁶ The binding of L-BABP in different proportions produced a progressive decrease and a small shift to lower temperature in the sharper peak and an increase in the broad components above 24 °C. The pretransition at 18 °C was absent in the lipid–protein complexes. The onset of the sharp calorimetric peak at lower temperature was coincident, both in the pure lipid and in the lipid–protein complexes, with the chain melting evidenced by the steep change in the stretching band of $-\text{CH}_2-$ (Figure 2). The temperature range for the transition detected by infrared spectroscopy spanned the whole range of the transition detected by DSC. Not enough resolution in the temperature axis in the FTIR experiment was achieved to detect two components that could be associated with the components detected by DSC. If the calorimetric components actually have different lipid chain organization, then it was only evidenced by a slight broadening

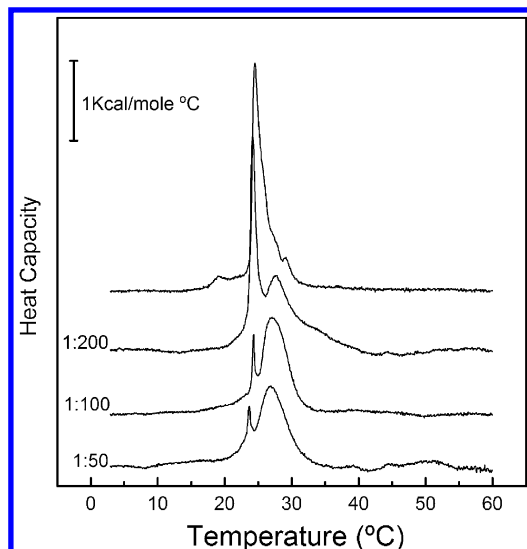


Figure 6. Differential scanning calorimetry of DMPG in the absence (top line) and in the presence of different amounts of L-BABP. The Figure shows the heat capacity as a function of the temperature after subtraction of solvent baseline. Samples contained 0.1 M NaCl, 0.4 mM DMPG, and 0, 2, 4, or 8 μ M L-BABP. Lipid/protein ratios for each experimental condition are shown next to the thermograms.

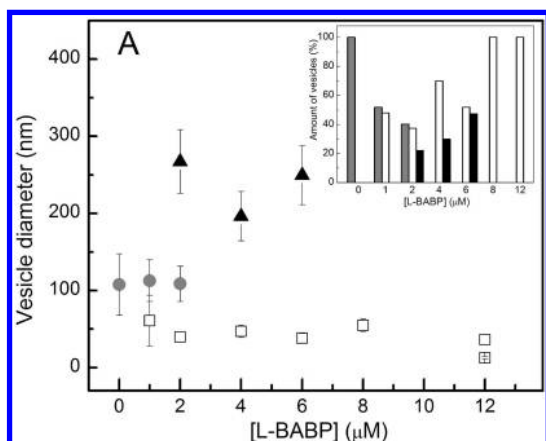


Figure 7. Size distribution of vesicles measured by dynamic light scattering. Protein was added stepwise to the sample containing DMPG vesicles in 0.1 M NaCl to reach concentrations from 0.5 to 12 μ M. Lipid concentration was 0.4 mM. Data correspond to the volume weighted distributions in Multimodal Nicomp analysis. The variety of vesicle sizes were grouped in vesicles of \sim 110 (gray circle and gray bars), <60 (\square and white bars), and >200 nm (\blacktriangle and black bars). The insert shows the relative amount of the different group of vesicles sizes under each condition.

of the transition detected by infrared spectroscopy. The same observation is valid for the conformational transition of L-BABP detected by FTIR.

Dynamic light scattering measurements showed that the addition of L-BABP to unilamellar DMPG vesicles produced changes in the size of the vesicles. Figure 7 shows that pure DMPG LUVs were of an average size of 110 nm in gel phase (16 $^{\circ}$ C). The addition of L-BABP produced a complex transformation in the system. Fitting the autocorrelation function using the Nicomp software revealed the coexistence of particles of different size that changed as a function of protein concentration (Figure 7). We defined three groups according to the particle size: diameters of \sim 110, <60 , and >200 nm. The relative proportions of these populations under each experimental condition are shown in the insert in Figure 7. Most probably, the particles of reduced size, as compared with the pure vesicles,

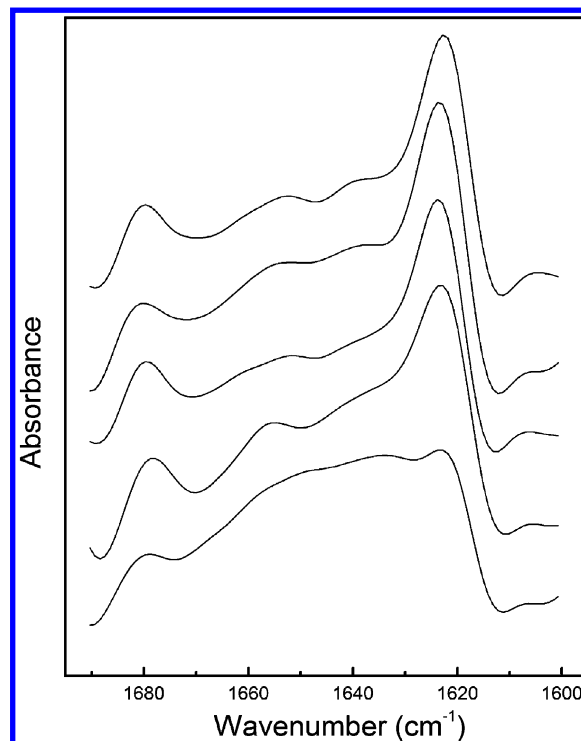


Figure 8. Fourier self-deconvolved spectra of L-BABP in different protein-lipid complexes. Spectra were taken from the series of measurements in Figures 2 and 4. Spectra were Fourier self-deconvolved using a $K = 2$ and $\text{fwhm} = 18 \text{ cm}^{-1}$ as in Nolan et al.⁶ From top to bottom L-BABP in solution at 16 $^{\circ}$ C, in the presence of DMPG at 16 $^{\circ}$ C, in solution at 37 $^{\circ}$ C, in the presence of DMPG-5% PC at 37 $^{\circ}$ C and in the presence of DMPG at 37 $^{\circ}$ C.

are still unilamellar vesicles, whereas the particles >200 nm could be the result of vesicles aggregation or vesicle fusion. This possibility was not further investigated.

Discussion

We observed different conformations of membrane-bound L-BABP depending on the composition of the lipid membrane, the lipid phase state, and the composition of the aqueous phase. In a previous work, we showed that at low ionic strength the membrane-bound protein was in a partially unfolded state when the lipid was in the gel phase, and a further unfolded state was acquired in the liquid-crystalline phase.⁷ Now we found that in the presence of 0.1 M NaCl also a native-like conformation of L-BABP can be stabilized when it is bound to lipids in the gel phases and also in lipids in the liquid-crystalline phase like POPG or DMPG containing 5% DMPC. Figure 8 shows the Fourier self-deconvolved spectra to illustrate and summarize these observations. It can be seen that some states of the membrane-bound protein have the same secondary structure as the native protein in solution, whereas under the condition of higher electrostatic surface potential, the secondary structure was largely changed. Still, in this unfolded state, some secondary structure is conserved, as evidenced by the presence of bands at 1627 and 1680 cm^{-1} , as described in our previous work.⁶ When L-BABP was bound to DMPG, DPPG, DMPA, and DPPA, the transition to the liquid-crystalline phase produced an unfolding of the protein, demonstrating that the mechanism is rather general and not specific for a particular lipid.

Several physical properties of the interface that change with the phase state of the lipid can mediate the modulation of the protein conformation. Because electrostatic interactions are

driving forces for the binding of L-BABP, we explored the changes in surface potential as possible triggers of protein unfolding at the interface. We measured the electrokinetic surface potential, ζ , of LUVs of POPG and DMGP membranes at different temperatures and considered ζ to be a good approximation for the surface potential, ψ_0 . For POPG membranes, we found small variation with the temperature, whereas a large increase in ζ was observed for DMPG in the liquid-crystalline as compared with the gel phase. Alternatively, when comparing ζ potential values of POPG and DMPG membranes, both at the same temperature and in the liquid-crystalline phase, the trend (a decrease in the ζ potential in POPG) was expected according to an increase in molecular area and consequently a decrease in the surface charge density.

Regarding the physical basis for the change in electrostatic surface potential in the lipid phase transition, several studies indicated that it could be the result of the balance of opposing factors. On one hand, the increase in lipid molecular area should produce a decrease in the surface density area in the expanded, liquid-crystalline phase as compared with the more condensed gel phase.²⁷ On the other hand, it was proposed that the affinity of Na^+ counterion for the phospholipid headgroup decreases in the liquid phase.²⁸ Because the counterion is more dissociated, the surface potential in the liquid phase should be larger. Actually, Riske et al.²⁸ have shown that a soluble cationic spin probe increases the partition into the interface of anionic lipid membranes of DMPG in the liquid phase as compared with the gel phase, and it can be directly explained by an increased surface potential. Our results are in accordance with these findings because we effectively found an increase in ζ potential of DMPG membranes after lipid melting. The fact that metal ions bind more strongly to the lipids in the gel phase is also supported by the observations of Binder and Zschörnig in phosphatidylcholine membranes.²⁹ In addition, the effect of surface hydration should also be considered. Tightly bound water in lipid polar head groups can modulate the dipole and surface potential. It has been proposed that water content in the membrane varies with the phase state of the lipid, giving an alternative explanation for the increment in ζ potential in the liquid phase.³⁰

We found a correlation between ζ potential, the membrane binding constants, and the protein conformation in the interface. For the pure lipids DMPG and POPG, the bound, native-like states corresponded to low values of the binding constant and low values of ζ potential, whereas the bound, unfolded state was observed only in the system with higher binding constant and ζ potential, that is DMPG in the liquid phase. Therefore, the acquisition of an unfolded state in the interface correlates with the increase in electrostatic surface potential. A rather small proportion of 5% of DMPC in liquid DMPG membranes decreased the ζ potential of these interfaces to the value corresponding to DMPG in the gel phase and shifted the state of the bound unfolded protein to native-like, bound state. This result, together with the occurrence of a native-like membrane-bound protein in liquid POPG membranes, clearly indicates that the native-like, membrane-bound state of L-BABP not only occurs in lipids in the gel phase but also can be stabilized in other lipid membranes with low electrostatic surface potential. These results indicate that protein conformation at membrane interface can be modulated by electrostatic surface potential. Therefore, changes in protein conformation coupled to lipid phase transitions can result as a consequence of the modification of electrostatic surface potential during lipid melting.

It is not surprising that an electric field can influence the conformation of the protein in the interface. The most immediate explanation is that the interaction of the electric field with molecular dipoles induces changes in vibrational modes and forces that lead to molecular rearrangement. This has been shown in molecular dynamic simulations of lysozyme in oscillating electromagnetic fields,³¹ in an amyloid peptide in an external constant field,³² and in our simulations of L-BABP both in an external electric field and within the field of the charged membrane.²⁵ Changes in the secondary structure due to interactions with an electric field have also been recently demonstrated for lysozyme in solution using circular dichroism and Raman spectroscopy.³³

Membrane electrostatic surface potential has been largely recognized as a driving force for the protein binding to lipid membrane,³⁴ acting as a factor that increases the protein concentration within the interface. Nevertheless, surface potential can also act directly on protein conformation. Astumian^{34,35} previously proposed theoretical models for the translocation and conformational shifts of membrane proteins driven by the electrophoretic movement of charged residues within the membrane electric field. Nevertheless, few experimental works have shown the direct dependence or correlation of the conformation of peripheral proteins with the membrane electrostatic potential. Membrane electric field, for example, was explicitly proposed as a determinant for conformational change of cytochrome *c* in the lipid membrane.³⁶ Besides, this protein is the only previous example of peripheral or nonintegral proteins in which conformational changes are clearly coupled to the lipid phase transition: it loses tertiary structure without noticeable changes in the secondary structure in a process coupled to the lipid phase transition, as revealed by the increase in proton–deuterium exchange.³⁷ In this regard, L-BABP is one of the very few examples in which protein conformational changes are directly correlated with changes in membrane surface potential and lipid phase state.

It can be considered that the global free energy of binding is contributed by at least two terms: the local increase in protein concentration in the interface due to the electrostatic surface potential and an intrinsic binding constant that includes short-range interactions between protein residues and phospholipids (both local electrostatics and van der Waals interactions), free energy due to the protein conformational change, and free energy of lipid rearrangement. The magnitude of these two components can be estimated. Column 6 in Table 1 shows the values of the effective binding free energy calculated from the experimental values of the binding constants. The contribution to the binding free energy due to Poisson–Boltzmann accumulation was calculated according to $zF\Psi_0$, where z is the net electrical charge of the species that concentrates in the interface, F is the Faraday constant, and Ψ_0 is the electrostatic surface potential. Ψ_0 was approximated to the measured electrokinetic surface potential, ζ . This expression actually applies to a small ion of charge z and does not exactly apply to the protein: the large exclusion volume of the protein precludes from reaching the interfacial concentration dictated by Boltzmann distribution for a point charge. Also, because of the large size, the charge on the protein is distributed along a spatial dimension of about the same size as the thickness of the electric double layer. As a consequence, the effective z value should be smaller than the expected value of +5 for L-BABP. We show the term $zF\Psi_0$ evaluated for $z = +1$ and $+5$ in columns 8 and 9, respectively, in Table 1. Even if the protein is “feeling” the whole value of surface potential and is displaying the full expected positive charge, the contribu-

tion of electrostatic concentration would be lower than the total free energy of binding. We conclude that other terms contributed to the binding free energy besides the Boltzmann concentration.

The finding that the calorimetric profile and size of the aggregates were changed upon binding of L-BABP indicates that the changes in the lipid order should also be included as a driving force for the binding of L-BABP. Despite the clear and simple correlation between protein conformational change and the changes in lipid chains order upon lipid phase transition, the system revealed a remarkable complexity regarding thermotropic behavior and long-range organization for DMPG/L-BABP complexes. Increasing the protein concentration produced an increase in a component of the thermotropic transition of DMPG above 24 °C and a decrease in the sharp peak at 24 °C. Clearly, the lipid components responsible for the heat absorption are in a dynamic exchange, and their relative amounts can be shifted by binding of L-BABP. A question that arises is whether the components of the thermotropic transition are laterally segregated phases within the same structure or separate structures, as for example vesicles of different sizes. DLS measurements at 16 °C show that increasing the protein concentration produced an increase in the population of small aggregates. Then, it can be proposed that the binding of L-BABP to DMPG membranes induces the formation of smaller vesicles with higher transition temperature. It must be noticed that the sharp peak at 24 °C was shifted to lower temperature with increasing amount of protein. This strongly suggests that this component is not pure lipid but contains bound protein. The shift to lower transition temperature indicates that L-BABP has larger affinity for the fluid phase of this component.

Our present findings contribute to explain the action mechanism of L-BABP. Two previous key findings largely helped us to understand the physiological role of this protein: the natural ligand is cholic acid,⁸ and the conformational change in the interface modulates the capacity to uptake and release the ligand in the membrane environment.⁹ The capacity of the lipid membrane to promote unfolding of L-BABP and the increased stability of the folded state by the binding of a ligand set the basis of a mechanism that determine whether the release or the uptake of ligand occurs in a determined cell microenvironment. Within this context, our results evidenced that the quality of the lipid membrane can modulate the ligand transfer activity of the protein. Here we demonstrated that relatively small changes in local lipid composition in the lipid membrane could easily modulate the strength of binding, the conformation in the interface, and consequently the affinity for the ligand.

Conclusions

We studied the conformations of L-BABP bound to anionic lipid membranes. The secondary structure of the protein was evaluated by the spectral shape of the infrared amide I' band. When L-BABP was bound to lipids with saturated acyl chains in the gel phase, the secondary structure was equal to the native structure in solution. The transition to the liquid-crystalline phase produced a conformational change in the membrane-bound protein leading to an unfolded or partially unfolded conformation. This was observed with anionic phospholipids with different polar headgroup and different melting transition temperature, indicating that it is a general dependence with the lipid phase state and not a specific behavior in a particular lipid membrane. Because increased surface potential (due to the melting of DMPG) conducted to an unfolded state and decreases in surface potential (whether by including DMPC in a DMPG membrane or by using POPG in liquid-crystalline state)

produced a native-like protein, we concluded that the electrostatic surface potential is the most probable physical factor that determines the conformation of L-BABP in the lipid interface. It is remarkable that subtle changes in the properties of the interface can shift conformations in an already membrane-bound protein. As a general conclusion, we shown that the conformation of a protein peripherally bound to anionic lipid membranes can be modulated in a more or less direct way by the physical state of the lipid acyl chains.

Acknowledgment. We thank Dr. Carla Giacomelli, Dpt. Physical Chemistry, FCQ UNC, for kindly allowing us to use the Delsa Nano C equipment and to Nucleoeléctrica Argentina S.A. Central Nuclear Embalse, Div. Química y Procesos for the kind donation of D₂O. This work was supported with grants from CONICET, SECYT UNC, and FONCYT. The Biocrystallography Laboratory of the University of Verona is funded by a grant from the Italian Ministry of Education and Scientific.

References and Notes

- (1) Seelig, J. Thermodynamics of lipid-peptide interactions. *Biochim. Biophys. Acta* **2004**, *1666*, 40–50.
- (2) Kloczek, G.; Schulthess, T.; Shai, Y.; Seelig, J. Thermodynamics of melittin binding to lipid bilayers. Aggregation and pore formation. *Biochemistry* **2009**, *48*, 2586–2596.
- (3) White, S. H.; Wimley, W. C. Membrane protein folding and stability: physical principles. *Annu. Rev. Biophys. Biomol. Struct.* **1999**, *28*, 319–365.
- (4) Ladokhin, A. S.; White, S. H. Folding of amphipathic α -helices on membranes: energetics of helix formation by melittin. *J. Mol. Biol.* **1999**, *285*, 1363–1369.
- (5) Johnson, J. E.; Cornell, R. B. Amphitropic proteins: regulation by reversible membrane interactions (review). *Mol. Membr. Biol.* **1999**, *16*, 217–235.
- (6) Nolan, V.; Perduca, M.; Monaco, H. L.; Maggio, B.; Montich, G. G. Interactions of chicken liver basic fatty acid-binding protein with lipid membranes. *Biochim. Biophys. Acta* **2003**, *1611*, 98–106.
- (7) Decca, M. B.; Perduca, M.; Monaco, H. L.; Montich, G. G. Conformational changes of chicken liver bile acid-binding protein bound to anionic lipid membrane are coupled to the lipid phase transitions. *Biochim. Biophys. Acta* **2007**, *1768*, 1583–1591.
- (8) Nicheola, D.; Perduca, M.; Capaldi, S.; Carrizo, M. E.; Righetti, P. G.; Monaco, H. L. Crystal structure of chicken liver basic fatty acid-binding protein complexed with cholic acid. *Biochemistry* **2004**, *43*, 14072–14079.
- (9) Pedo, M.; Lohr, F.; D'Onofrio, M.; Assfalg, M.; Dotsch, V.; Molinari, H. NMR studies reveal the role of biomembranes in modulating ligand binding and release by intracellular bile acid binding proteins. *J. Mol. Biol.* **2009**, *394*, 852–863.
- (10) Zhang, Y. P.; Lewis, R. N.; McElhaney, R. N. Calorimetric and spectroscopic studies of the thermotropic phase behavior of the n-saturated 1,2-diacylphosphatidylglycerols. *Biophys. J.* **1997**, *72*, 779–793.
- (11) Riske, K. A.; Döbereiner, H. G.; Lamy-Freund, M. T. Gel-fluid transition in dilute versus concentrated DMPG aqueous dispersions. *J. Phys. Chem. B* **2001**, *106*, 239–246.
- (12) Heimburg, T.; Biltonen, R. L. Thermotropic behavior of dimyristoylphosphatidylglycerol and its interaction with cytochrome *c*. *Biochemistry* **1994**, *33*, 9477–9488.
- (13) Schneider, M. F.; Marsh, D.; Jahn, W.; Kloege, B.; Heimburg, T. Network formation of lipid membranes: triggering structural transitions by chain melting. *Proc. Natl. Acad. Sci. U.S.A.* **1999**, *96*, 14312–14317.
- (14) Riske, K. A.; Amaral, L. Q.; Döbereiner, H. G.; Lamy, M. T. Mesoscopic structure in the chain-melting regime of anionic phospholipid vesicles: DMPG. *Biophys. J.* **2004**, *86*, 3722–3733.
- (15) Alakoskela, J. M.; Kinnunen, P. K. Thermal phase behavior of DMPG: the exclusion of continuous network and dense aggregates. *Langmuir* **2007**, *23*, 4203–4213.
- (16) Scapin, G.; Spadon, P.; Pengo, L.; Mammi, M.; Zanotti, G.; Monaco, H. L. Chicken liver basic fatty acid-binding protein (pI 9.0). Purification, crystallization, and preliminary X-ray data. *FEBS Lett.* **1988**, *240*, 196–200.
- (17) Hope, M. J.; Bally, M. B.; Cullis, P. R. Production of large unilamellar vesicles by a rapid extrusion procedure. Characterization of size distribution, trapped volume and ability to maintain a membrane potential. *Biochim. Biophys. Acta* **1985**, *812*, 55–65.
- (18) Bartlett, G. R. Phosphorus assay in column chromatography. *J. Biol. Chem.* **1959**, *234*, 466–468.

- (19) Arrondo, J. L.; Castresana, J.; Valpuesta, J. M.; Goni, F. M. Structure and thermal denaturation of crystalline and noncrystalline cytochrome oxidase as studied by infrared spectroscopy. *Biochemistry* **1994**, *33*, 11650–11655.
- (20) Garidel, P.; Richter, W.; Rapp, G.; Blume, A. Structural and morphological investigations of the formation of quasi-crystalline phases of 1,2-dimyristoyl-*sn*-glycero-3-phosphoglycerol (DMPG). *Phys. Chem. Chem. Phys.* **2001**, *3*, 1504–1513.
- (21) Snyder, R. G. Vibrational study of the chain conformation of the liquid *n*-paraffins and molten polyethylene. *J. Chem. Phys.* **1967**, *46*, 1316–1360.
- (22) Casal, H. L.; Mantsch, H. H. Polymorphic phase behaviour of phospholipid membranes studied by infrared spectroscopy. *Biochim. Biophys. Acta* **1984**, *779*, 381–401.
- (23) Surewicz, W. K.; Leddy, J. J.; Mantsch, H. H. Structure, stability, and receptor interaction of cholera toxin as studied by Fourier transform infrared spectroscopy. *Biochemistry* **1990**, *29*, 8106–8111.
- (24) Lewis, R. N.; McElhaney, R. N.; Pohle, W.; Mantsch, H. H. Components of the carbonyl stretching band in the infrared spectra of hydrated 1,2-diacylglycerol bilayers: a reevaluation. *Biophys. J.* **1994**, *67*, 2367–2375.
- (25) Villarreal, M. A.; Perduca, M.; Monaco, H. L.; Montich, G. G. Binding and interactions of L-BABP to lipid membranes studied by molecular dynamic simulations. *Biochim. Biophys. Acta* **2008**, *1778*, 1390–1397.
- (26) Riske, K. A.; Amaral, L. Q.; Lamy, M. T. Extensive bilayer perforation coupled with the phase transition region of an anionic phospholipid. *Langmuir* **2009**, *25*, 10083–10091.
- (27) Trauble, H.; Eibl, H. Electrostatic effects on lipid phase transitions: membrane structure and ionic environment. *Proc. Natl. Acad. Sci. U.S.A* **1974**, *71*, 214–219.
- (28) Riske, K. A.; Nascimento, O. R.; Peric, M.; Bales, B. L.; Lamy-Freund, M. T. Probing DMPG vesicle surface with a cationic aqueous soluble spin label. *Biochim. Biophys. Acta* **1999**, *1418*, 133–146.
- (29) Binder, H.; Zschornig, O. The effect of metal cations on the phase behavior and hydration characteristics of phospholipid membranes. *Chem. Phys. Lipids* **2002**, *115*, 39–61.
- (30) Disalvo, E. A.; Lairion, F.; Martini, F.; Tymczyszyn, E.; Frias, M.; Almaleck, H.; Gordillo, G. J. Structural and functional properties of hydration and confined water in membrane interfaces. *Biochim. Biophys. Acta* **2008**, *1778*, 2655–2670.
- (31) English, N. J.; Mooney, D. A. Denaturation of hen egg white lysozyme in electromagnetic fields: a molecular dynamics study. *J. Chem. Phys.* **2007**, *126*, 091105-1–091105-5.
- (32) Toschi, F.; Lugli, F.; Biscarini, F.; Zerbetto, F. Effects of electric field stress on a β -amyloid peptide. *J. Phys. Chem. B* **2009**, *113*, 369–376.
- (33) Zhao, W.; Yang, R. Experimental study on conformational changes of lysozyme in solution induced by pulsed electric field and thermal stresses. *J. Phys. Chem. B* **2010**, *114*, 503–510.
- (34) Westerhoff, H. V.; Tsong, T. Y.; Chock, P. B.; Chen, Y. D.; Astumian, R. D. How enzymes can capture and transmit free energy from an oscillating electric field. *Proc. Natl. Acad. Sci. U.S.A* **1986**, *83*, 4734–4738.
- (35) Tsong, T. Y.; Astumian, R. D. Electroconformational coupling and membrane protein function. *Prog. Biophys. Mol. Biol.* **1987**, *50*, 1–45.
- (36) Muga, A.; Mantsch, H. H.; Surewicz, W. K. Membrane binding induces destabilization of cytochrome *c* structure. *Biochemistry* **1991**, *30*, 7219–7224.
- (37) Heimburg, T.; Marsh, D. Investigation of secondary and tertiary structural changes of cytochrome *c* in complexes with anionic lipids using amide hydrogen exchange measurements: an FTIR study. *Biophys. J.* **1993**, *65*, 2408–2417.

JP104035Z